

17th World Conference on Earthquake Engineering, 17WCEE
Sendai, Japan - September 13th to 18th 2020

FLOOR-DIAPHRAGM ANCHORAGE SYSTEM FOR SEISMIC RESISTANT BUILDINGS WITH ENHANCED RELIABILITY

G. Tsampras[1], J.I. Restrepo[2], R. Sause[3], R.B. Fleischman[4], Z. Zhang[5]

[1] *Falcon Vehicle Structures Engineer, SpaceX, tsampras.g@gmail.com*
[2] *Professor, University of California San Diego, jrestrepo@ucsd.edu*
[3] *Professor, Lehigh University, rs0c@lehigh.edu*
[4] *Professor, University of Arizona, rfleisch@email.arizona.edu*
[5] *Senior Engineer, Thornton Tomasetti, zzhang@thorntontomasetti.com*

Abstract

This paper presents an innovative anchorage system that connects the floor-diaphragm with the lateral force resisting system (LFRS) of a seismic resistant building. The anchorage system was developed through an integrated numerical and experimental research program funded by the U.S. National Science Foundation and the Network for Earthquake Engineering Simulation. The anchorage system is deformable and allows relative displacement between the floor and the LFRS. It consists of a limited-strength load-carrying hysteretic component (friction device or a buckling-restrained brace), low damping rubber bearings, and bumpers. The force-deformation response of the limited-strength load carrying hysteretic component is designed to limit the earthquake induced horizontal inertial forces transferred from the floor to the LFRS. The rubber bearings provide additional post-elastic stiffness to the anchorage system and out of plane stability to the LFRS. The bumpers limit the potential impact forces and the relative displacement between the floor and the LFRS under maximum considered earthquake events. A full-scale experimental program was conducted at the Advanced Technology for Large Structural Systems engineering research center at Lehigh University and validated the force-deformation response of the components of the anchorage system. A shake-table experimental program was conducted at the Large High-Performance Outdoor Shake Table at the University of California San Diego to assess the seismic response of a half-scale, four-story reinforced concrete flat-plate shear wall building that includes the anchorage system. The shake-table experimental results show that the anchorage system can limit the seismic response of the building and potentially minimize the damage of structural and non-structural components. Results from numerical simulations of a twelve-story reinforced concrete shear wall building model subjected to design basis earthquake ground motions show that the use of the anchorage system enhances the reliability of a building structure against earthquakes by reducing the sensitivity of building's structural response to the variations of the characteristics of the earthquake ground motions.

Keywords: shake table; experiments; floor accelerations; buckling restrained braces; friction devices



1. Introduction

In a conventional earthquake-resistant building system, the gravity load resisting system (GLRS) includes the floor system, where most of the seismic mass is located, and the floor system is rigidly attached to the lateral force resisting system (LFRS), which resists the earthquake-induced horizontal inertial forces generated by the acceleration of the seismic mass [1][2]. It has been shown that the seismic inertial forces generated in the floor system can be large relative to the floor diaphragm strength, and can lead to inelastic and potentially non-ductile response of the diaphragm [3]. The development of excessive inertial forces due to high floor accelerations can produce nonlinear response and serious damage of the LFRS, which may lead to unsatisfactory seismic response [4] [5]. The nonlinear response of the LFRS can act as a "cut–off" mechanism that may limit the floor accelerations [6] [7] [8]. However, even when ductile nonlinear response of the LFRS occurs, high floor accelerations may be observed, due to the response contribution of second and higher modes [7] [9]. Studies of LFRS with a predominantly flexural response (e.g. a reinforced concrete cantilever structural wall), which is dominated by nonlinear moment-rotation response at the base of the LFRS, show that high floor accelerations due to the second-mode and higher-mode response can be expected [10] [11] [12] [13] [14] [15]. The kinematic interaction between the LFRS and the floor systems is also expected to increase the overturning moment capacity and the shear force demand in the LFRS [15].

An innovative anchorage system between the floor system of a flexible GLRS and the stiff LFRS of an earthquake-resistant building used to limit the earthquake-induced horizontal inertial forces was presented in [16] [17] [18]. The anchorage system is deformable and allows relative displacement between the floor and the LFRS. It consists of a limited-strength load-carrying hysteretic component (friction device or a buckling-restrained brace), low damping rubber bearings, and bumpers. The combination of the limited strength hysteretic component and the low damping rubber bearings are termed as deformable connection. Figure 1 shows a schematic example of the anchorage system that includes the deformable connection installed in a reinforced concrete shear wall earthquake-resistant building. Floor openings are introduced around the LFRS (i.e., shear-walls). The force-deformation response of the limited-strength load carrying hysteretic component is designed to limit the earthquake induced horizontal inertial forces transferred from the floor to the LFRS. The compressive stiffness of the rubber bearings ensures the out-of-plane stability of the LFRS. The shear stiffness of the rubber bearings provides additional post-elastic stiffness to the deformable connection. The vertical motion of the LFRS at each floor level is constrained only by the shear stiffness of the rubber bearings connecting the plane of the LFRS with the floor system. The bumpers limit the potential impact forces and the relative displacement between the floor and the LFRS under maximum considered earthquake events.

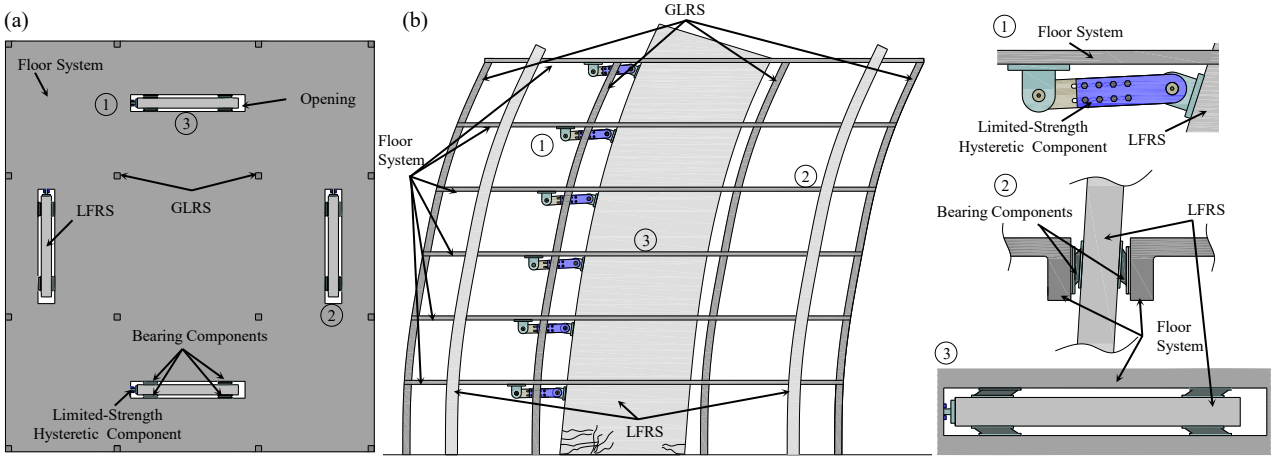


Fig. 1: Sketches of an earthquake-resistant building system with deformable connections.

© The 17th World Conference on Earthquake Engineering



This paper presents experimental results from a full-scale experimental program that was conducted at the Advanced Technology for Large Structural Systems engineering research center at Lehigh University. The tests validated the force-deformation response of the deformable connection of the anchorage system. Two configurations of the deformable connection were tested. The first configuration of the deformable connection consists of a buckling restrained brace (BRB) and steel-reinforced low damping laminated rubber bearings, and it is denoted as BRB+RB [19]. The second configuration of the deformable connection consists of a friction device (FD) and carbon fiber-reinforced low damping laminated rubber bearings, and it is denoted as FD+RB [20]. Results from a shake-table experimental program that was conducted at the Large High-Performance Outdoor Shake Table at the University of California San Diego are presented, as well. The shake-table test assessed the seismic response of a half-scale, four-story reinforced concrete flat-plate shear wall building that includes the anchorage system. Limited results from numerical simulations of a twelve-story reinforced concrete shear wall building model subjected to design basis earthquake ground motions are presented. The journal papers [18, 19, 20, 21] include a detailed discussion of the research findings summarized in this paper.

2. Full-scale component experimental testing

2.1 Experimental set-up

Figure 2 shows the experimental set-up used to test the BRB+RB and the FD+RB connections. A simulated floor system and a reinforced concrete shear wall (i.e., the LFRS) were built in the laboratory. The experimental set-up was designed to test the force-deformation response of the deformable connections subjected to quasi-static and dynamic displacement histories. A detailed description of the test set-up is presented in [19] [20] [22]. The same experimental set-up was used to separately evaluate the force-deformation response of the bumpers [23].

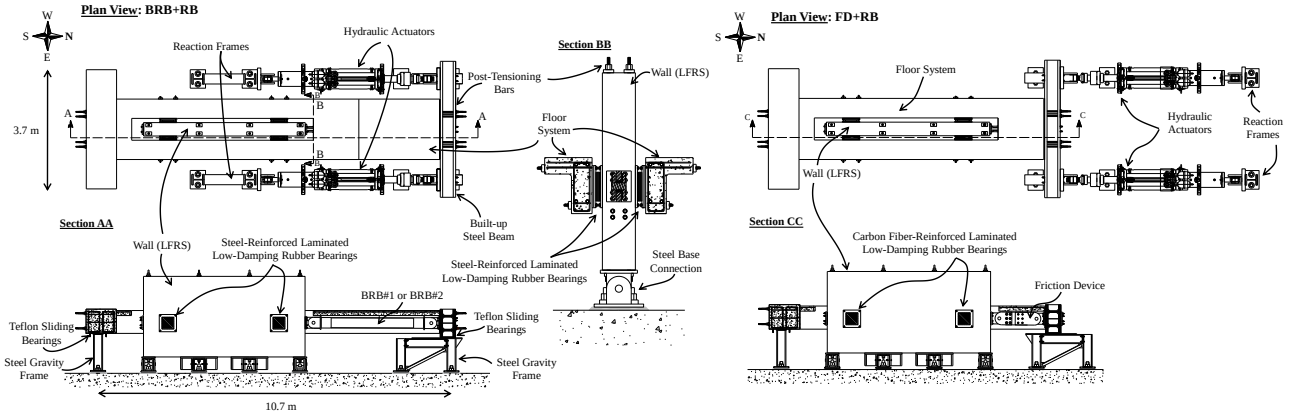


Fig. 2: Full-scale test set-up of BRB+RB and FD+RB connections.

2.2 Buckling-restrained brace

Two BRB+RB connections were tested using two identical BRBs and one set of four steel-reinforced low damping rubber bearings. Figure 3(a) shows the BRB components and Figure 3(b) shows one of the two BRBs installed in the experimental set-up. BRB#1 and BRB#2 had the same nominal dimensions and material properties. Table 1 lists key dimensions of the BRBs. Symbols *t*, *b*, and *L* with the appropriate subscript denote the thickness, width, and length respectively of the yielding zone, transition zone, knife plates, and clevis plates. The yielding zone steel material was ASTM A36 steel. One yielding zone plate was used. L_{yz} was determined from the 2.2% axial strain design limit, assuming the BRB design deformation demand equals 50 mm.

© The 17th World Conference on Earthquake Engineering



Table 1 - BRB component dimensions

Yielding Zone			Transition Zone			Knife Plates			Clevis Plates		
t_{yz} [mm]	b_{yz} [mm]	L_{yz} [m]	t_{tz} [mm]	b_{tz} [mm]	L_{tz} [mm]	t_{kp} [mm]	b_{kp} [mm]	L_{kp} [mm]	t_c [mm]	b_c [mm]	L_c [mm]
25.4	139.2	2.3	25.4	250.4	398.8	38.1	330.2	368.3	63.5	330.2	374.7

The steel modulus of elasticity E_s, the nominal material yielding stress F_{yn}, the actual material yield stress F_{ya} (based on steel coupon test results provided by the BRB manufacturer), the expected nominal yielding force $P_{by,n}$, the expected actual yielding force $P_{by,a}$, and the material overstrength factor R_y (equal to the ratio of F_{ya} to F_{yn}) are given in Table 2. Figure 3(c) shows the pin load cell used to measure the force in the BRB. Figure 3(d) and (e) show the linear variable displacement transducers (LVDTs) used to measure the axial deformation of the BRB.

Table 2 - Material properties and strength of BRB yielding zone

Material	E_s [GPa]	F_{yn} [MPa]	F_{ya} [MPa]	$P_{by,n}$ [kN]	$P_{by,a}$ [kN]	$R_y = F_{ya}/F_{yn}$ [-]
ASTM A36	200	248	282	876	996	1.14

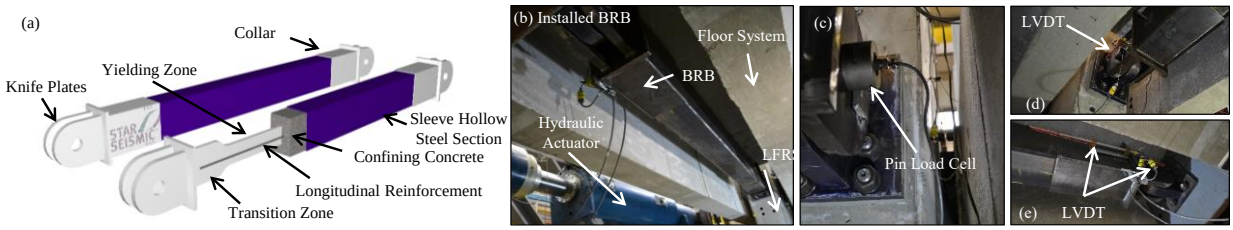


Fig. 3: (a) Components of BRB; (b) BRB in test set up; (c), (d), (e) BRB instrumentation.

2.3 Friction device

Figure 4 shows the full-scale FD and its components. Two outer steel plates, one middle steel plate, and two friction shims are clamped using ASTM A325 bolts that are denoted as “friction bolts”. The FD has two friction (sliding) interfaces between the middle steel plate and the two friction shims. The friction bolts pass through standard holes in the outer steel plates and the friction shims. These standard holes have 1.6-mm (i.e., 1/16-inch) larger diameter than the diameter of the friction bolts. Slots in the middle steel plate allow the friction bolts, the outer steel plates, and the friction shims to move relative to the middle steel plate (sliding occurs between the friction shims and the inner steel plate). Clevis plates with spherical bearings were used to accommodate the kinematic requirements and to prevent out-of-plane forces (acting normal to the sliding interfaces) from developing in the FD. The FD is symmetric about the longitudinal axis to prevent out-of-plane forces from developing in the FD.

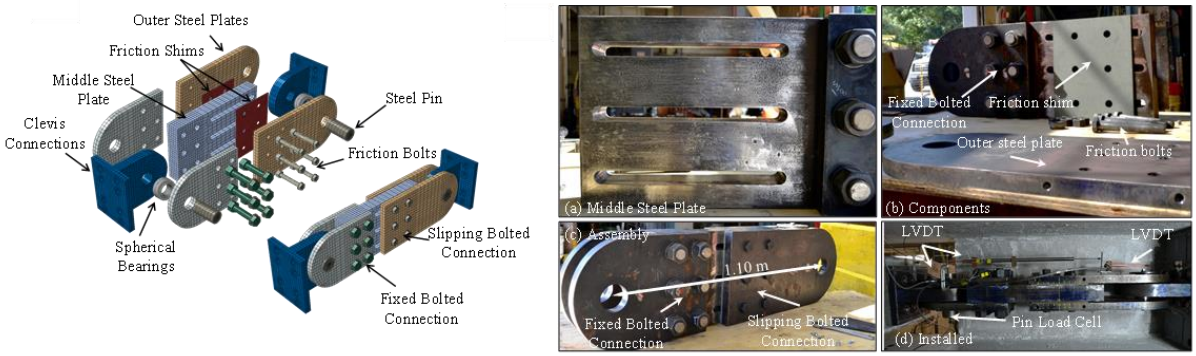


Fig. 4: Schematic of full-scale FD components; and (a) Middle steel plate; (b) Other FD components; (c) Assembled FD; (d) Instrumentation of installed FD.

© The 17th World Conference on Earthquake Engineering



Figure 4(d) shows the pin load cell used to measure the force in the FD and the LVDTs used to measure the axial deformation and sliding of the FD. The FD design deformation is close to 100 mm. The friction force can be estimated using Coulomb theory, $F_s = n_s N \mu_s$, where $n_s = 2$ is the number of friction interfaces, N is the total normal force that the friction bolts apply on the friction interfaces, and μ_s is the friction coefficient. Six ASTM A325 25.4-mm diameter friction bolts were used. The friction shims were made of the composite material Gatke 398 [24] and the μ_s assumed to be 0.45. The target friction force in the tests discussed in this paper was 735 kN. Additional tests are discussed in [20] [22].

2.4 Low-damping laminated rubber bearings

Two different types of low-damping laminated rubber bearings were tested. One set of four steel-reinforced low-damping laminated rubber bearings was used in the BRB#1+RB and BRB#2+RB connections. One set of four carbon fiber-reinforced low-damping laminated rubber bearings was used in the FD+RB connection. The rubber was 50+/-5 Duro Gr. 3 with estimated shear modulus G = 0.9 MPa, based on the upper bound of G provided by AASHTO [25]. Table 3 lists the dimensions and the expected properties of the each rubber bearing based on the estimated G. W and L are the plan dimensions of the rubber, A is the area of the rubber WL, h_{rt} is the total thickness of the four rubber layers, n_L is the number of rubber layers, S is the shape factor of the rubber layers, K_{RB} is the elastic shear stiffness of the rubber bearing, E_c is the compressive modulus of the rubber bearing, and K_c is the compressive stiffness of the rubber bearing. The expected total shear stiffness of the four rubber bearings is $4K_{RB}$ = 8.8 kN/mm. In the experiments, the total rubber bearings shear force in the four rubber bearings was measured indirectly by subtracting the force measured in the BRB load cell from the sum of the forces in the two actuators.

Table 3 - Dimensions and nominal properties of each rubber bearing.

W	L	h_{rt}	n_L	$h_{ri}=h_{ri}/n_L$	$S=A/[2h_{ri}(W+L)]$	G	$K_{RB}=GA/h_{rt}$	$E_c=6GS^2$	$K_c=E_cA/h_{rt}$
[mm]	[mm]	[mm]	[-]	[mm]	[-]	[MPa]	[kN/mm]	[MPa]	[kN/mm]
356	356	50	4	12.5	7.0	0.9	2.2	264	656

Note: Area of the rubber $A=WL$

2.5 Experimental results

Figure 5 shows deformation and force time histories of the BRB+RB and the FD+RB connections due to quasi-static and dynamic sinusoidal displacement histories, and quasi-static earthquake displacement histories. The time has been normalized with respect to the total time of each test. The test number is shown on x-axis.

Test 1 was the first test of BRB#1+RB. Test 10 was the first test of BRB#2+RB. One set of four steel-reinforced rubber bearings was used in Tests 1 through 18. The steel-reinforced rubber bearings had been subjected to limited deformation cycles prior to Test 1.The Gatke398 friction shims were new at the beginning of Test 30. One set of four carbon fiber-reinforced rubber bearings was used in Tests 30 through 45. The carbon fiber-reinforced rubber bearings had been subjected to significant deformation cycles prior to Test 30 while testing other types of friction shims.

The BRB+RB and the FD+RB connections had stable and repeatable hysteretic force-deformation responses under many deformation cycles. The FD+RB post-elastic force-deformation response was controlled by the FD friction force, the effects of the sliding history on the FD friction force, and the RB force-deformation response. The peak FD+RB force under dynamic loading was approximately 15% less than the peak FD+RB force under quasi-static loading. The BRB+RB post-elastic force-deformation response was controlled by the yielding force of the BRB, the isotropic hardening of the BRB, the dynamic effects on the BRB force-deformation response, and the RB force-deformation response. The dynamic and quasi-static peak BRB+RB forces were similar.

© The 17th World Conference on Earthquake Engineering



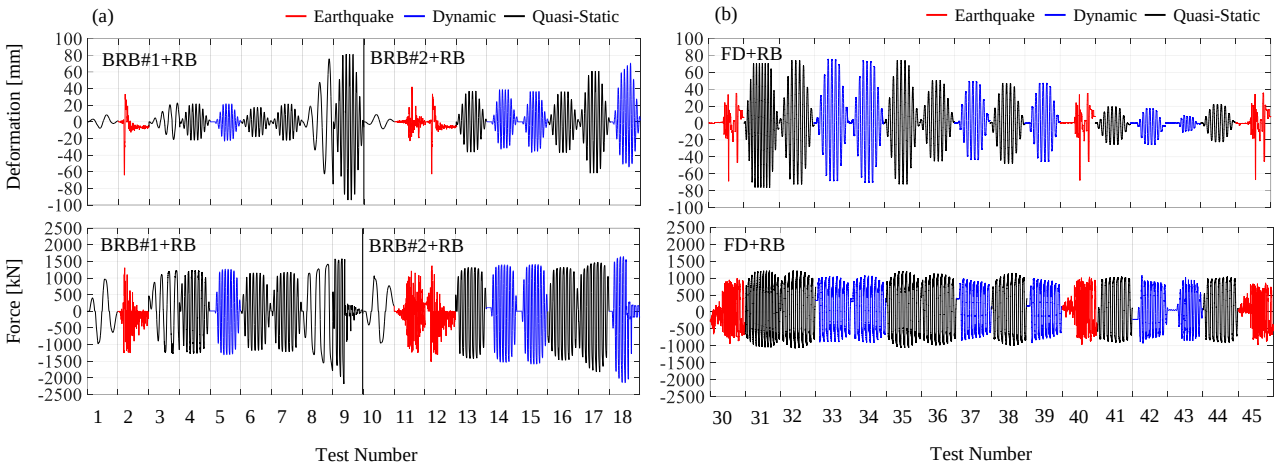


Fig. 5: Force and deformation normalized time histories for (a) BRB+RB and (b) FD+RB connections.

Figure 6(a) shows a large amplitude (compared to the 50mm BRB design limit) quasi-static force-deformation response of the FD and the BRBs. The FD elastic stiffness was approximately 1730 kN/mm. The FD had a friction-Coulomb type nonlinear hysteretic force-deformation response. The "break-in" effect, the sliding history, and the dwell time affected the FD friction force [20]. As a result, the FD friction force varied from the target friction force by approximately +/- 15% [20]. The BRB elastic stiffness was approximately 185 kN/mm. Thus, the BRB+RB elastic stiffness was approximately 10 times smaller than the FD+RB elastic stiffness. The BRB had a smooth transition from elastic to post-elastic force-deformation response (i.e., Bauschinger effect). The BRB post-elastic force response is mainly controlled by the BRB isotropic hardening. The BRB isotropic hardening depends on the maximum plastic deformation range experienced by the BRB yielding zone [19]. The BRB kinematic hardening in compression is larger than the BRB kinematic hardening in tension. The difference is mainly due to friction from contact of the yielding zone with the confining concrete when the BRB was in compression and the Poisson's effect [27]. The isotropic and kinematic hardening in the BRB force-deformation response results in significant overstrength that needs to be considered for the design of the clevis connections.

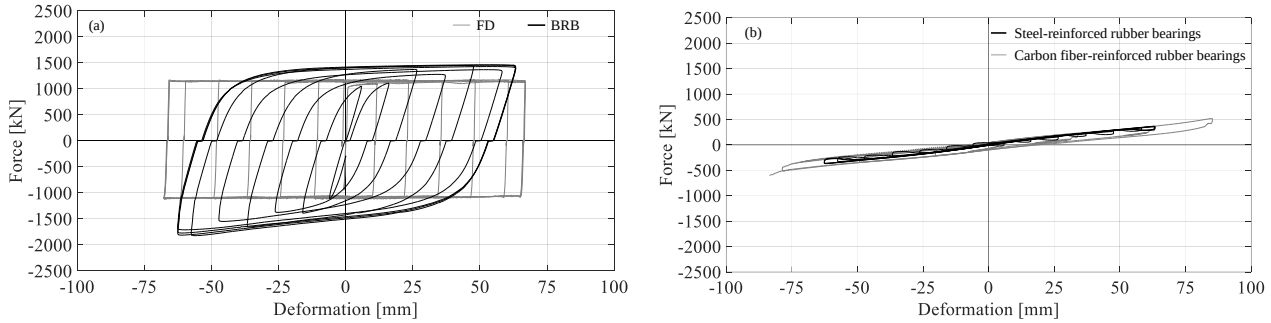


Fig. 6: (a) Typical quasi-static force-deformation response of BRB connection and FD connection. (b) Typical shear force-deformation response of steel-reinforced low damping rubber bearings and carbon fiber-reinforced low damping rubber bearings.

Figure 6(b) shows the typical quasi-static force-deformation response of steel-reinforced low-damping laminated rubber bearings from initial tests of BRB#1+RB and carbon fiber-reinforced low-damping laminated rubber bearings from initial FD+RB tests prior to test 30. Both types of rubber bearings had approximately linear-elastic response with negligible hysteretic behavior compared to the behavior of the FD and the BRB. The effective stiffness of the steel-reinforced rubber bearings and the carbon fiber-reinforced rubber bearings during the first large deformation tests was approximately 6.5 kN/mm.

© The 17th World Conference on Earthquake Engineering



Figure 7 shows that the quasi-static force-deformation response of the FD+RB connection, the FD, the steel-reinforced rubber bearings, the BRB+RB connection, the BRB, and the carbon fiber-reinforced rubber bearings. The post-elastic stiffness of the FD+RB is determined based on the effective stiffness of the steel-reinforced rubber bearings. The effective stiffness of the carbon fiber-reinforced rubber bearings contributes to the BRB+RB post-elastic stiffness. The post-elastic stiffness of the deformable connections is important to limit their deformation demand.

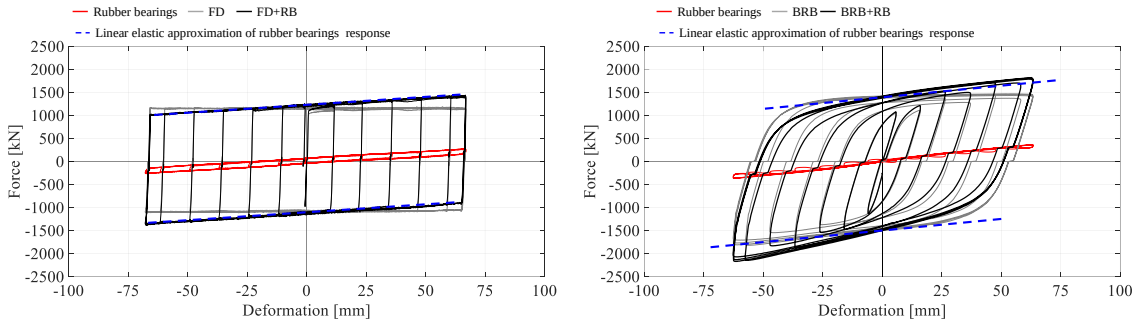


Fig. 7: Typical quasi-static force-deformation response of BRB+RB connection, FD+RB connection, and their components.

Figure 8 shows typical quasi-static and dynamic force-deformation responses of the deformable connections. Under dynamic loading the BRB+RB force increased up to 15% compared to the BRB+RB force under quasi-static loading because the BRB force increases as the instantaneous deformation rate increases [19]. The peak BRB+RB force is similar for the quasi-static and dynamic sinusoidal loading because the instantaneous deformation rate is almost zero at peak deformation. Under dynamic loading the FD+RB force decreased up to 15% compared to the FD+RB force under quasi-static loading because the FD force decreases as the maximum (over the displacement history) peak sliding velocity of the FD increases [20].

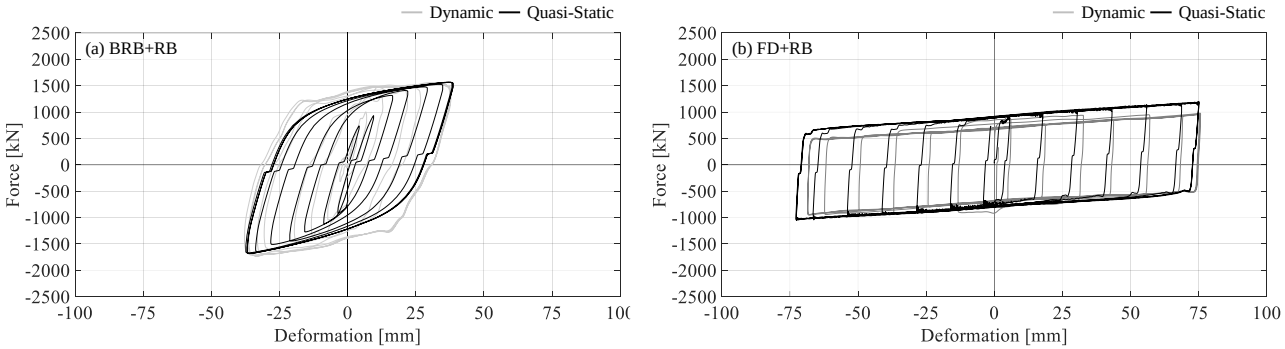


Fig. 8: Comparison of typical quasi-static and dynamic force-deformation responses of (a) BRB+RB connection and (b) FD+RB connection.

3. Shake-table experimental testing

3.1 Experimental set-up

The shake-table experimental testing program was conducted at the Large High-Performance Outdoor Shake Table at the University of California San Diego to assess the seismic response of a half-scale, 4- story reinforced concrete flat- plate shear wall building that includes the anchorage system [21]. Precast hybrid rocking walls and special precast columns were used for test repeatability in a 22-input strong ground-motion sequence. Figure 9 shows the sketch model of the building tested on the shake-table, the

© The 17th World Conference on Earthquake Engineering



northwest view of the building, and sketches of the anchorage system used in the building. The building was purposely designed with an eccentric wall layout to examine the performance of the system in coupled translational-torsional response. The building was tested in three phases to assess the effectiveness of the use of the anchorage system compared to conventional systems. In phase I, the floors were connected to the LFRS using the anchorage system. In Phase II, the floors were "locked" down to the walls to simulate a conventional floor anchorage in order to provide a direct comparison with Phase I. In Phase III, the walls were "locked" into the foundations. Thus, the rocking walls in Phase III are fixed at their base. This allows the comparison of a fixed base reinforced concrete shear wall structure with the response of the structures tested in Phase I and Phase II.

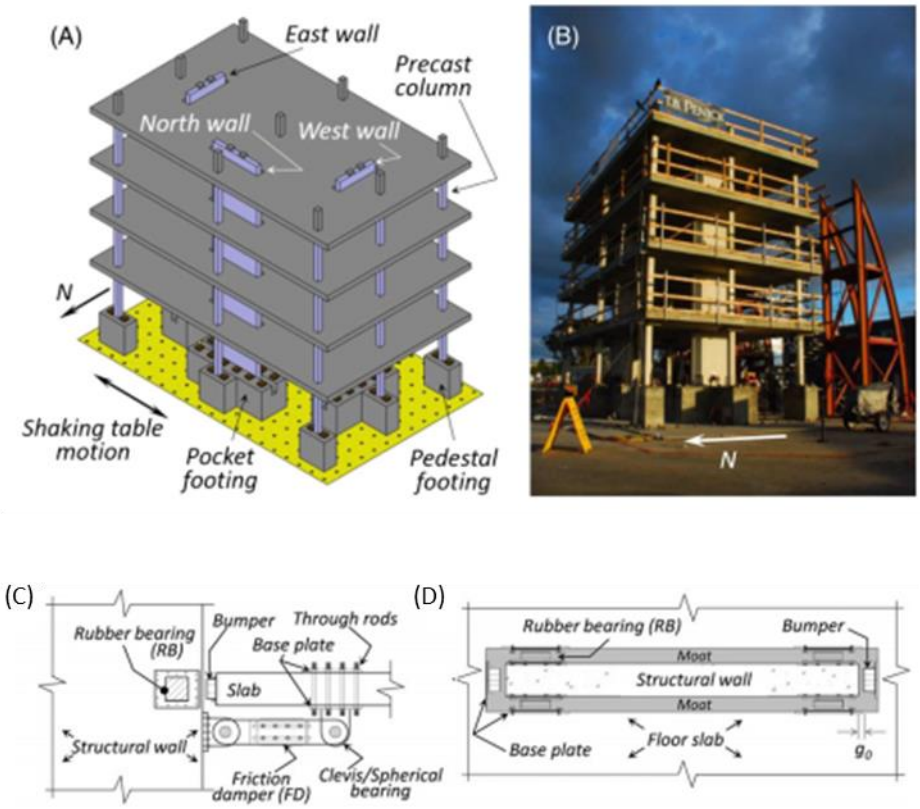


Fig. 9: Test structure: Isometric model view (A); View from northwest (B); Elevation (C) and plan view (D) of the anchorage system installed in the shake-table test. [21]

3.2 Experimental results

The shake-table test results confirmed that the components of the anchorage system ensure the reliable transfer of the inertial forces from the floors to the LFRS under complex three-dimensional kinematics. At a building system level, the shake-table test results demonstrated that the anchorage system tested in Phase I can reduce the seismic demand in the LFRS compared to the building with the conventional floor anchorage system tested in Phase II. More specifically, the test results showed that the use of the anchorage system that includes the deformable connection can lead to reduced shear wall base rotation, as shown in Figure 10. Additionally, the use of the anchorage system that includes the deformable connection can lead to reduced shear wall and column inter-story drift, and, in some cases, reduced floor accelerations. Furthermore, the use of the anchorage system that includes the deformable connection reduced the torsional response of the building structure. These results indicate the potential for the anchorage system that includes

© The 17th World Conference on Earthquake Engineering



the deformable connection to minimize damage to the primary structural and non-structural components during earthquakes.

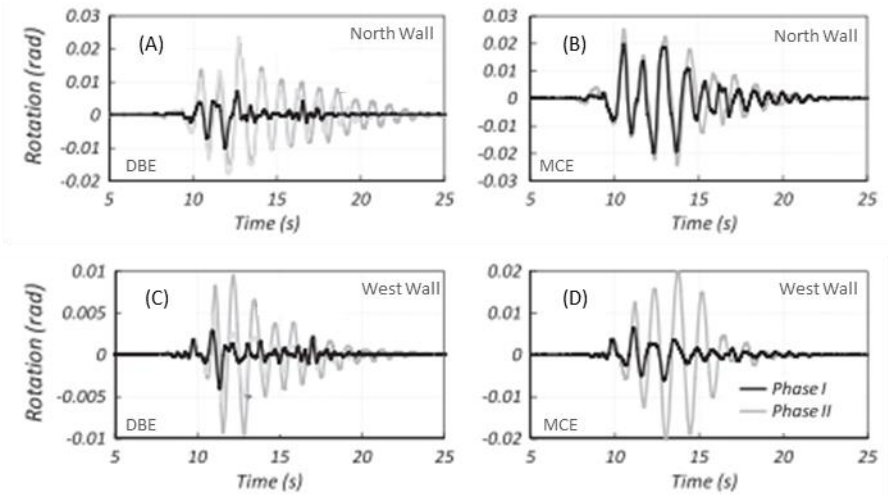


Fig. 10: Comparison of the in-plane rotation at the base of the north and west walls under a design basis earthquake (DBE) and a maximum considered earthquake (MCE) in phase I and phase II of the test [21].

4. Numerical simulations

Earthquake numerical simulations of a twelve-story reinforced concrete shear wall building structure were conducted to compare the seismic response of the building structure that included the anchorage system that consisted of the BRB+RB or the FD+RB connections with the seismic response of the building structure that included a rigid elastic connection between the floors and the shear-walls [18]. The numerical building models were subjected to eighteen ground motions scaled to match the spectral accelerations of the ASCE7-10 [26] design basis earthquake spectrum over a range of periods T∈ [0.6, 2.0] seconds. Figure 11(a) shows that the peak shear force (V_{LFRS}) in the shear wall for the systems with the anchorage system are reduced in every story compared with the system with rigid elastic connections. The dispersion of the peak V_{LFRS} around the mean peak value is smaller for the systems with anchorage system. Figure 11(b) shows the peak connection force (F_c) transferred from the floor systems to the LFRS. The use of the anchorage system successfully limits the peak F_c, the mean peak values of F_c at each floor are similar, and the dispersion of the peak F_c is significantly reduced. The results from the numerical simulations demonstrate that the use of the anchorage system can significantly enhance the reliability of the building system against earthquake ground motions by reducing the sensitivity of the building's structural response to the variations of the characteristics of the earthquake ground motions.

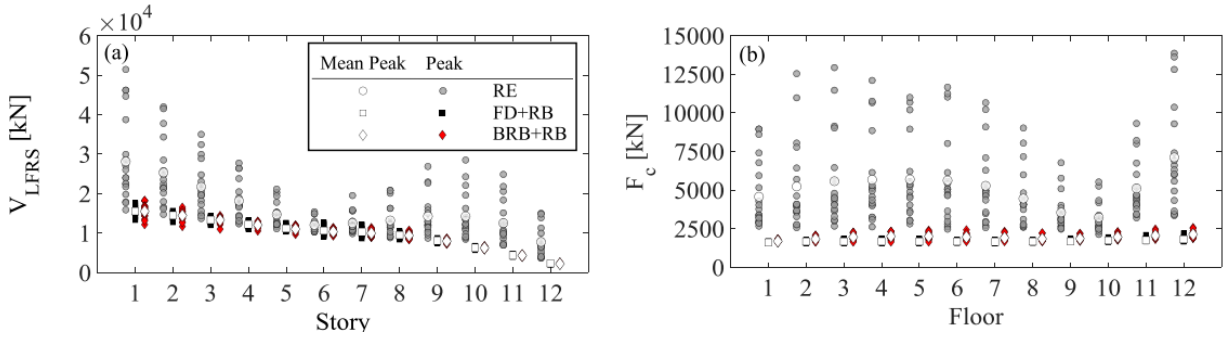


Fig. 11: Peak and mean peak story shears and connection forces at each story/floor; RB, low damping laminated rubber bearings; BRB, buckling restrained brace; FD, friction device; RE, rigid elastic [18].

© The 17th World Conference on Earthquake Engineering



5. Conclusions

This paper presented an innovative anchorage system that connects the floor-diaphragm with the lateral force resisting system (LFRS) of a seismic resistant building. A full-scale component experimental testing program validated the force-deformation response of the components of the anchorage system. A shake-table experimental testing program showed that the anchorage system can limit the seismic response of the building and potentially minimize the damage of structural and non-structural components. Numerical simulation results of a twelve-story reinforced concrete shear wall building subjected to design basis earthquake ground motions showed that the use of the anchorage system enhances the reliability of a building structure against earthquakes by reducing the sensitivity of building's structural response to the variations of the characteristics of the earthquake ground motions.

6. Acknowledgements

This paper is based upon work supported by grants from National Science Foundation, Award No. CMMI-1135033 in the George E. Brown, Jr. Network for Earthquake Engineering Simulation Research (NEESR) program, and Award No. CMMI-0402490 for the George E. Brown, Jr. Network for Earthquake Engineering Simulation (NEES) consortium operations. The authors are grateful for additional financial support provided by the Gerondelis Foundation, Yen Fellowship, and Lehigh University. The contributions of the NEES@Lehigh staff, the ATLSS Center staff, and the NEES@UCSD staff are acknowledged. Any opinions, findings, and conclusions expressed in this report are those of the authors and do not necessarily reflect the views of the National Science Foundation or others acknowledged here.

7. References

[1] J. P. Moehle, J. D. Hooper, D. J. Kelly and T. R. Meyer "Seismic design of cast-in-place concrete diaphragms, chords, and collectors," National Institute of Standards and Technology, 2010.

[2] R. Sabelli, T. A. Sabol and S. W. Easterling, "Seismic design of composite steel deck and concrete-filled diaphragms," National Institute of Standards and Technology, 2011.

[3] R. Fleischman and K. Farrow, "Dynamic behavior of perimeter lateral-system structures with flexible diaphragms," Earthquake Engineering and Structural Dynamics, vol. 30, no. 5, pp. 745-763, 2001.

[4] M. Rodriguez, J. Restrepo and A. Carr, "Earthquake - induced floor horizontal accelerations in buildings," Earthquake Engineering and Structural Dynamics, pp. 693-718, 2002.

[5] M. Rodriguez, J. Restrepo and J. Blandon, "Seismic design forces for rigid floor diaphragms in precast concrete building structures," Journal of Structural Engineering, pp. 1604-1615, 2007.

[6] T. Kelly, "Floor response of yielding structures," Bulletin of New Zealand National Society for Earthquake Engineering, pp. 255-272, 1978.

[7] S. Ray-Chaudhuri and T. Hutchinson, "Effect of nonlinearity of frame buildings on peak horizontal floor acceleration," Journal of Earthquake Engineering, pp. 124-142, 2011.

[8] F. X. Flores, D. Lopez-Garcia and F. A. Charney, "Assessment of floor accelerations in special steel moment frames," Journal of Constructional Steel Research, vol. 106, pp. 154-165, 2015.

[9] R. Sewell, A. Cornell, G. Toro and R. McGuire, "A study of factors influencing floor response spectra in nonlinear multi-degree-of-freedom structures," The John A. Blume Earthquake Engineering Center Report No. 82, 1986.

[10] A. K. Chopra, Dynamics of Structures, Berkeley,CA, California: Pearson Prentice Hall, 2007.

[11] D. Roke, "Damage-free seismic-resistant self-centering concentrically-braced frames," Ph.D. Dissertation, Lehigh University, Bethlehem,PA, 2010.

[12] A. D. Amaris Mesa, "Dynamic amplification of seismic moments and shear forces in cantilever walls," M.Sc. Thesis, University of Pavia, Pavia, 2002.

© The 17th World Conference on Earthquake Engineering



[13] L. Wiebe and C. Christopoulos, "Mitigation of higher mode effects in base-rocking systems by using multiple rocking sections," Journal of Earthquake Engineering, pp. 83-108, 2009.

[14] L. Wiebe, C. Christopoulos, R. Trembley and M. Leclere, "Mechanisms to limit higher mode effects in a controlled rocking steel frame. 1: Concept, modelling, and low-amplitude shake table testing," Earthquake Engineering and Structural Dynamics, pp. 1053-1068, 2013.

[15] M. Panagiotou, J. I. Restrepo and J. P. Conte, "Shake-table test of a full-scale 7-story building slice. Phase I: Rectangular wall," Journal of Structural Engineering, vol. 137, no. 6, pp. 691-704, 2011.

[16] D. Zhang, R. Fleischman and Z. Zhang, "Analytical Investigation of Seismic Behavior of Building Structures with an Inertial Force-Limiting Floor Anchorage System," International Journal of Engineering and Technology, vol. 8, no. 4, pp. 234-240, 2016.

[17] R. Fleischman, J. Restrepo, A. Nema, D. Zhang, U. Shakya, Z. Zhang, R. Sause, G. Tsampras and G. Monti, "Inertial Force-Limiting Anchorage System for Seismic Resistant Building Structures," in Structures Congress 2015, Portland, OR, 2015.

[18] G. Tsampras, R. Sause, D. Zhang, R. B. Fleischman, J. I. Restrepo, D. Mar and J. Maffei, "Development of deformable connection for earthquake-resistant buildings to reduce floor accelerations and force responses," Earthquake Engineering and Structural Dynamics, vol. 45, no. 9, p. 1473–1494, 2016.

[19] G. Tsampras, R. Sause, R. Fleischman and J. Restrepo, "Experimental study of deformable connection consisting of buckling-restrained brace and rubber bearings to connect floor system to lateral force resisting system," Earthquake Engineering & Structural Dynamics, vol. 46, no. 8, pp. 1287-1305, 2016.

[20] G. Tsampras, R. Sause, R. Fleischman and J. Restrepo, "Experimental study of deformable connection consisting of friction device and rubber bearings to connect floor system to lateral force resisting system," Earthquake Engineering & Structural Dynamics, 2017, DOI: 10.1002/eqe.3004.

[21] Z. Zhang, R. Fleischman, J. Restrepo, G. Guerrini, A. Nema, D. Zhang, U. Shakya, G. Tsampras and R. Sause, "Shake table test performance of an inertial force-limiting floor anchorage system", *Earthquake Engineering & Structural Dynamics*, vol. 47, no. 10, pp. 1987-2011, 2018, https://doi.org/10.1002/eqe.3047.

[22] G. Tsampras and R. Sause, "Development and experimental validation of deformable connection for earthquake-resistant building systems with reduced floor accelerations," Network of Earthquake Engineering Simulation (NEES) Technical Report, https://nees.org/resources/13612, 2015

[23] Z. Zhang, Analytical investigation of inertial force-limiting floor anchorage system for seismic resistant building structures, Dissertation, The University of Arizona, 2017

[24] Scan Pan Inc., "Gatke Material Selection Guide," Menomonee Falls, WI, USA, 2010.

[25] AASHTO, LRFD Bridge Design Specification, Washington, DC, 2010.

[26] ASCE. ASCE Standard ASCE/SEI7 – 10: Minimum Design Loads for Buildings and Other Structures. American Society of Civil Engineers: Reston, Virginia, 2010

[27] B. Saxey and M. Daniels, "Characterization of overstrength factors for buckling restrained braces," in *Proceedings in Australian Structural Engineering Conference 2014*, Auckland, NZ, 2014

© The 17th World Conference on Earthquake Engineering